Research Article | Vol. 27, No. 3 | 4 Feb 2019 | OPTICS EXPRESS 3746
Optics EXPRESS

Designing a hydraulic support system for large monolithic mirror's precise in-situ testing-polishing iteration

HAIFEI HU,[1,2,*] XIAO LUO,[2] ZHENYU LIU,[2] XUEJUN ZHANG,[2] DONGLIN XUE,[2] AND HONGWEI ZHAO[1]

[1]*School of Mechanical and Aerospace Engineering, Jilin University, Changchun, Jilin 130022, China*
[2]*Changchun Institute of Optics, Fine Mechanics and Physics, Chinese Academy of Sciences, Changchun, Jilin 130033, China*
**huhf@ciomp.ac.cn*

Abstract: In order to improve the fabrication efficiency and testing accuracy of meter-scale, large monolithic mirrors, hydraulic support units (HSUs) are commonly used. However, the challenges to reduce the disparity of the HSUs' stiffness and keep the stability of the mirrors' altitude are hard to resolve, especially for large-scale mirrors. In this paper, we found the air ratio of the working fluid for HSUs is a key factor for designing the HSUs to resolve the challenges from the analytical solution that we derived for supporting large mirrors. Here we designed, tested and fabricated dozens of HSUs and used a four-meter SiC mirror, the world's largest monolithic SiC reported in public, as a study case. It shows that the stiffness values of grouped HSUs vary within ± 3%, and the mirror's reference surface PV is less than 20 μm in 10 days, producing a mirror tip/tilt angle less than 1.5″. The surface error of the supported mirror is about 20 nm, which is very close to the ideal case where uniform stiffness exists, for randomly distributed stiffness values. The repeatability of the in-situ interferometric test with 0.019 λ RMS of the mirror surface demonstrates the supporting system in a high precision. With such a supporting system, the fabrication process of this mirror was estimated to be sped up by 47% compared to the typical fabricating iteration. With minor modifications and easy extensions, such a novel supporting system could be used widely for many in-situ, high-quality fabricating-testing processes.

1. Introduction

Comparing to traditional optical materials, SiC has an excellent performance regarding on the specific stiffness, thermal stability, heat conductivity and lightweight performance, which appears intensive interests of fabricating SiC mirrors around the world [1–5]. After several decades of development, SiC mirrors have been widely used in meter-scale telescopes, especially for the space-based or large ground-based telescopes, whose weights are the dominant challenges for manufacturing and installation process [2–4]. To achieve high resolution of observation, large primary mirrors, which are usually the heaviest components among the whole telescope system are preferred by the scientists and engineers [5,6]. However, for such giant mirrors, one of the challenging tasks is to design and assembly the support system for in situ polishing and testing [7].

Comparing to the traditional fabricating process for large mirrors, the fabricating and measuring process are the separating and independent procedure. The workpiece will be moved from the machining platform to a horizontal testing table for precise surface measurement [8,9]. Such off-line measurement process will inevitably cause additional measurement uncertainty, as well as additional workloads, which become a critical issue on the time schedule and budget [8,10,11]. It will become a key challenge when the mirror is up to 2-4 meter or even larger, considering the difficulties on handling and assembling it.

#352261 https://doi.org/10.1364/OE.27.003746
Journal © 2019 Received 22 Nov 2018; revised 6 Jan 2019; accepted 13 Jan 2019; published 1 Feb 2019

Optics EXPRESS

Therefore, an in situ testing approach arises, and has been adopted by many ongoing projects for large telescopes such as GMT and E-ELT [12–14]. For such kind of projects and in situ measuring strategy, the hydraulic/hydrostatic in situ support system (HISS) has been considered as the best solution for support platform for many large mirrors since the 1980s [15,16] owing to its stiffness merit for overcoming the print through effect during polishing [17,18].

However, the distortion effect on the mirror surface figure arises from the support units' stiffness disparity, and the stability of such system have not been studied yet. These factors become extremely important when the mirror requires a high precision with RMS<λ/30 (λ = 632.8 nm hereafter), or with a stable time <1 min after adjustment and a pressure change <0.1 kPa/s for keeping the mirror quasi-static during in situ testing, or in the case of that the mirror is relatively soft and thin [18]. To solve these problems, performance evaluation should be carefully investigated in the unit, group and system level. Some key points were found to be critical: (1) output force accuracy and the stiffness disparity for precision evaluation and prediction; (2) long time stability; (3) supported mirror surface figure accuracy. In this paper, we have addressed these issues theoretically and evaluated by the design and testing outputs.

2. Precision mechanism

In practice the HISS loop is recommended to be divided into several groups for mirror adjustment prior to testing, as shown in Fig. 1. Figure 1(a) illustrates a lightweight mirror supported by 4 groups consisting of several hydraulic support units (HSUs) from the mirror back-view, and Fig. 1(b) shows a typical group configuration within the HISS.

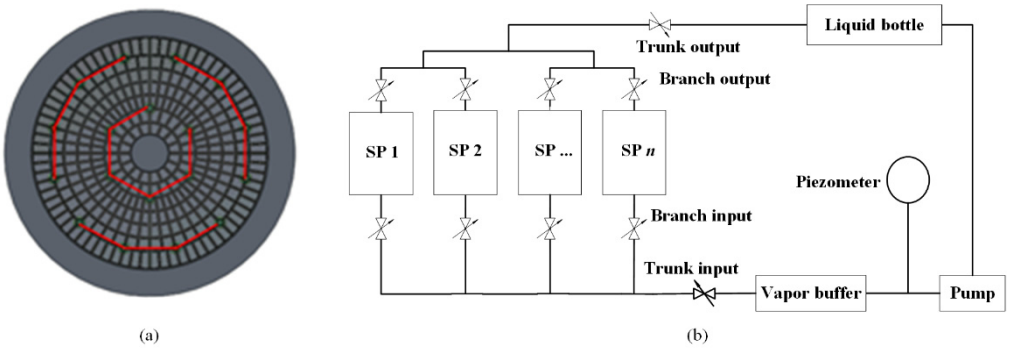

Fig. 1. HISS for testing-fabricating large mirrors: (a) system concept; (b) loop concept.

There are some basic principles for group division: (1) follow the opto-mechanical engineers' decision; (2) put the supports outputting the same force in the same group; (3) provide the function of workpiece adjustment. Usually the work fluid cycles within the pipe loop, delivered by the pump and purified by the vapor buffer bottle, and recycles to the liquid bottle. A piezometer is adopted to monitor the work pressure, a trunk valve is installed for the group input and output port respectively. For each HSU's input and output port, there is also a branch valve for quick repair or substitution. Additionally, the workpiece could be easily controlled by pre-calibrated pump's revolution-mirror latitude relationship.

2.1 HSU design and force accuracy

The HSU with the application of a single rolling diaphragm is designed and its section view is shown in Fig. 2. The mechanical components and the diaphragm forms a narrow inner space for the fluid to work in. When the space is filled with pressurized fluid, the diaphragm bears tensile load and rolls along the center-bottom fixed piston. With the assumptions that inner fluid pressure is P, the diaphragm's clearance C is relatively small compared to its radius R meanwhile relatively large compared to its thickness t ($10t \le C \le 0.1R$) and tensile stress is

Optics EXPRESS

uniformly distributed along t, the force balance of the bottom curved part magnified in detailed view I could be expressed as

$$2F = 2\pi R \cdot C \cdot P \tag{1}$$

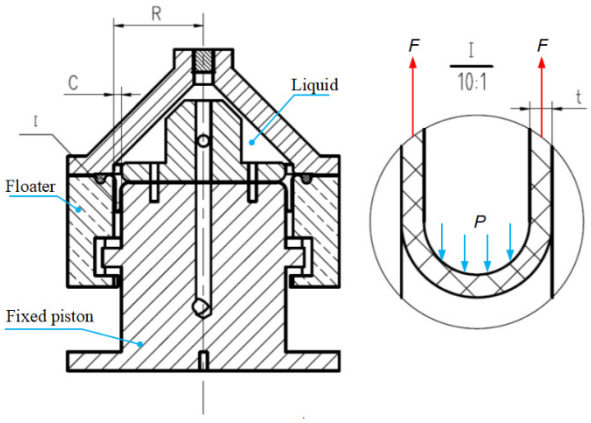

Fig. 2. HSU section view and the diaphragm's tensile force.

Where F is the diaphragm's tensile force of each ring of the diaphragm, as shown in Fig. 3, G is the gravity of the floater weighing m, F_{out} equals the HSU's output force applied to the mirror and F_P is the total force of inner pressure. For force balance, one has

$$F_P = F_{out} + F + G \tag{2}$$

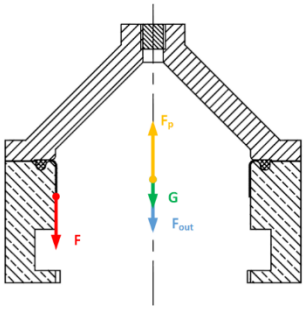

Fig. 3. Force balance of the HSU in pressurized state.

It's known that $G = mg$, $F_P = \pi R^2 P$ and from Eq. (1) one could get $F = \pi RCP$, so Eq. (2) becomes

$$\pi R^2 P = F_{out} + \pi RCP + mg \tag{3}$$

For evaluating the accuracy of F_{out}, a group consisting of 5 HSUs was tested as shown in Fig. 4(a), whose configuration is consistent with Fig. 1(b), where 5 units are linked end to end with a valve between neighboring units for flexible and fast grouping option. Displacement sensor was used for monitoring the HSU's top movement s, force sensor embedded in the machine beam records the support force F_{out} and the piezometer tells the real-time fluid pressure P. The stiffness test could be easily carried out by the Chinese National Standard testing machine DDL10. For controlling the air ratio within the fluid, a vapor buffer within the group illustrated in Fig. 1(b) is shown in Fig. 4(b). It's very important that: (1) one should always keep the fluid-vapor interface higher than the bottle's input and output; (2) the bottle should be installed closer to the units than the piezometer whose inner air ratio is hard to control.

Optics EXPRESS

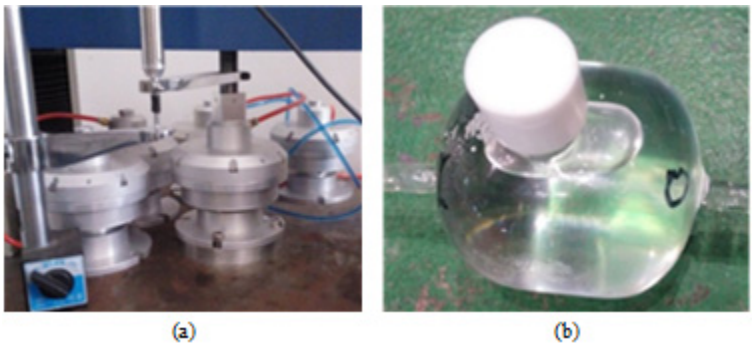

Fig. 4. Testing a 5-unit group: (a) group with 5 HSUs in test; (b) vapor buffer bottle.

The output forces of 5 units responding to different work pressure are recorded and summarized in Table 1. It's seen that the relative PV value between the 5 forces and their average F_{avg} distributes within 1.35% as the work pressure P ranges from 45 kPa to 78 kPa, and the 5 output forces become more uniform as the pressure increases. It's recommend that all the units work at as high pressure as possible on the premise that the diaphragm is safe enough.

Table 1. Force accuracy for 5 HSUs in group

P/kPa	F_{avg}/N	U_1(%)	U_2(%)	U_3(%)	U_4(%)	U_5(%)	PV(%)
45.07	292.8	–0.82	0.36	0.53	–0.53	0.46	1.35
50.33	327.1	–0.31	0.22	0.47	–0.63	0.25	1.10
56.07	364.2	0.04	0.09	0.42	–0.46	–0.09	0.98
62.27	403.8	0.09	0.20	0.52	–0.37	–0.44	0.96
68.20	442.5	0.04	0.10	0.42	–0.30	–0.26	0.72
72.28	469.3	0.30	0.02	0.32	–0.36	–0.28	0.68
78.28	507.0	–0.14	0.13	0.42	–0.25	–0.17	0.67

Especially, for the cases of P>56 kPa, which are for common applications, both the maximum and the minimum relative difference are smaller than 0.5%, one could regard all units within the same group as the equal-force type. According to this equal-force mechanism, the mirror would not deform uniformly if the HSU stiffness values are different from each other, which is inevitable in reality. So more attention is paid to the units' stiffness analysis in the next paragraph.

2.2 Stiffness disparity

The HSU only has axial stiffness, and it could be expressed as

$$S = \frac{\mathrm{d}F_{\mathrm{out}}}{\mathrm{d}s} \tag{4}$$

where $\mathrm{d}F_{\mathrm{out}}$ represents the change of output force, $\mathrm{d}s$ represents the floater motion. From Eq. (3), the former one could be rewritten as

$$\mathrm{d}F_{\mathrm{out}} = \pi R\left(R-C\right)\mathrm{d}P = -\pi R\left(R-C\right)K\frac{\mathrm{d}V}{V} \tag{5}$$

with

Optics EXPRESS

$$\mathrm{d}V = \pi RC\left(\frac{\mathrm{d}s + \mathrm{d}l}{2}\right) - \pi R^2 \mathrm{d}s \tag{6}$$

where K is the fluid bulk modulus and V is the working volume, l denotes the generatrix length of the diaphragm, loads dP and dF stretch l by dl with the floater moving downward by ds.

Omitting the derivation process (see Appendix), the HSU's stiffness could be calculated as

$$S = \frac{\pi^2 R^2 (R - C)(R - C/2)}{V/K + \pi RC^2 l/4Et} \tag{7}$$

where E is the effective elastic modulus of the diaphragm.

What's more, it's very common that the fluid involves some air bubble. Using Boyle's law on condition that the air temperature does not change, for the bubbles there is the relation

$$P_0^{\mathrm{a}} V_0^{\mathrm{a}} = C_0 \tag{8}$$

and the corresponding volume change of the air is

$$\mathrm{d}V^{\mathrm{a}} = V^{\mathrm{a}} - V_0^{\mathrm{a}} = -\frac{\mathrm{d}P\ V_0^{\mathrm{a}}}{P} \tag{9}$$

This volume is replaced by the fluid, with detailed derivation omitted (see Appendix), the support stiffness turns out to be

$$S = \frac{\pi^2 R^2 (R - C)(R - C/2)}{V^{\mathrm{f}}/K + \pi RC^2 l/4Et + V_0^{\mathrm{a}}/P} \tag{10}$$

From Eq. (10), the factors affecting the stiffness could be concluded as: (1) the geometrical dimension parameters, such as the unit's working radius R, clearance C and the diaphragm's generatrix length l and thickness t; (2) the material property parameters, such as the fluid's bulk modulus K and the diaphragm's effective elastic modulus E; (3) the volume parameters, V^{f} for the fluid and V_0^{a} for the air; and (4) the working pressure parameter P.

For the self-made HSU all parameters are given except the parameter V_0^{a}, which is unknown and hard to measure, so the stiffness test and prediction based on the test are to be carried out before use. Stiffness test could be carried out by the system shown in Fig. 4, and it follows the following procedures.

(1) Install the test units onto the test platform and link them together.

(2) Close the very valves to get specific type of hydraulic group.

(3) Move the machine's load beam slowly to initial work pressure (F_{out} ~300 N).

(4) Load the i th HSU to F_{out} = 500 N for n times.

(5) Take 20%-40% region of the F_{out} -s curve to calculate the stiffness S_{ij} of the j th test of unit i.

(6) Compute the average stiffness S_i as

$$S_i = \frac{1}{n}\sum_{j=1}^{n} S_{ij} \tag{11}$$

(7) Evaluate the group stiffness S_{E} by averaging all S_i and the relative stiffness difference of every unit $e_i = S_i$-S_{E}.

Optics EXPRESS

(8) Repeat the above procedures till all units are tested.

Results achieved by the above procedures are summarized in Table 2. It shows that the 5 stiffness values vary from 1890 to 2002 N/mm averaging 1944 N/mm. The stiffness of all units relatively varies within the region of ± 3%. This lays an important foundation of system performance evaluation later.

Table 2. Stiffness for grouped 5 HSUs at about 300 N

No.	n	S_i/N·mm^{-1}	$e_i = S_i$-S_E	e/S_E %
1	2	1935	–9.6	–0.5
2	4	1978	33.4	1.7
3	5	1918	–26.6	–1.4
4	3	2002	57.4	3.0
5	2	1890	–54.6	–2.8
Group average S_E		1945		

Furthermore, unit 3 in the group was isolated for single test at different load, and the results are shown in Table 3. It tells that the single unit stiffness ranges from 8.7 kN/mm to 16.2 kN/mm responding to output forces of 100-357 N. This implies that the unit's stiffness could be improved by times through working at higher pressure, which also means that if the output force is determined one could use smaller units provided that the diaphragm does not break. The single unit stiffness is 15.6 kN/mm when it independently carries 1/54 weight of the 4-m SiC mirror (F_{out} ~300 N).

Table 3. Stiffness test for 3# HSU at different load

F_{out}/N	100	200	245	300	357
S/ N·mm-1	8693	11113	13221	15588	16191

With the above stiffness values at different working volume, it's possible to estimate the air volume ratio with the help of Eq. (10). For selected given ratios of V_0^a and determined HSU design, one could draw a series of stiffness-volume curve for each air volume ratio α. Five such curves with α ranging from 0.04% to 0.24% are shown in Fig. 5.

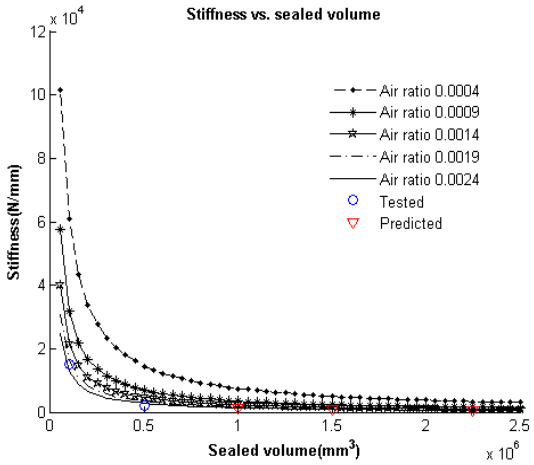

Fig. 5. Unit stiffness prediction of 3 types of group working for 4-m SiC mirror.

By plotting the two spots of 1.94 k at grouped 5 units' volume and 15.6 k at isolated 1 unit's volume, we could find the closest one of the five curves to them, then we could guess the value of V_0^a approximately. It's found that the two points locate nearest to the curve of α = 0.24%. With this input, stiffness prediction for any group with known work fluid volume becomes possible. Also S values of 3 types of group working for the coming 4-m mirror are predicted as 0.85 kN/mm, 1.1 kN/mm and 1.7 kN/mm respectively, as shown in Fig. 5.

This section lays a foundation for application of HISS to large mirrors.

3. Stability test

3.1 Group level stability

Two tests are performed to check the HSU group's stability at initial pressure near 90 kPa. They differ in initial test pressure, unit number and test time. As there are no output forces for the units, the force balance is automatically achieved through holding the floater by the fixed piston (see Fig. 2), with all diaphragms loaded. In such tests, the group stability could be investigated as well as the safety by monitoring the work pressure. The trends of pressure versus test time are plotted in Fig. 6.

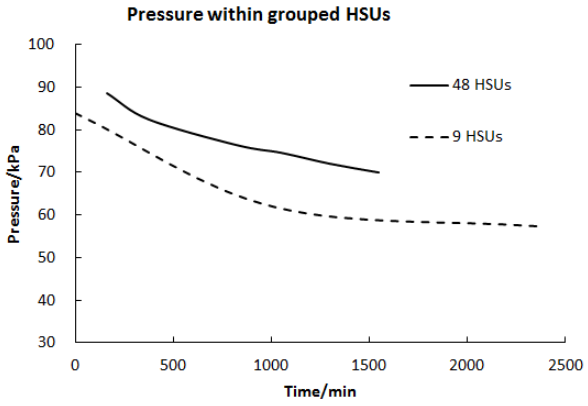

Fig. 6. Stability performance of unloaded hydraulic groups.

In the first test, 9 units are linked end to end, tests starts at about 84 kPa and lasts for about 2400 minutes. After the test lasts for 1000 minutes, the pressure changes much more slowly. So the next test is shortened to 1500 minutes with another 48 units involved starting from ~90 kPa.

Both of the tests experienced a pressure drop of about 20 kPa slowly. As the fluid volume within a single unit's is only about 100 ml, any leakage would cause significant pressure change in a second. From the curves in Fig. 6, it's seen that the pressure changes very slowly during a period of 0.5-1 day at a rate of 0.01 kPa/s, which is close to the piezometer's resolution.

Also it is discovered that the group consisting of more units has a stabler inner pressure. For most large mirrors, the number of units in a group ranges from 6 to 30, much like the tested typical groups. These results tell that all units are well sealed and they are stable enough in group level prior to the mirror installation.

3.2 System level stability

A dummy Φ4.08 m mirror weighing ~2 t is installed for system level stability verification. Based on the in situ testing data of self-made swing arm profilometer [19], three key points equally spaced along the circular direction at a radius of 2.02 m on the mirror's reference surface attracts special attention. The Z position of the three points in 8 testing-polishing iterations happened in about 10 days are plotted in Fig. 7.

It shows that the mirror has an absolute motion of ~40 μm, maybe caused by the polishing shop temperature change or environment vibration. What's more important is the relative altitude change of the three points, this could be represented by the PV value of them. The PV value also shows the mirror's tip/tilt change caused by polishing load, but it only had a value of less than 20 μm. For a mirror aperture of ~4 m, 20 um PV corresponds to a maximum

Optics EXPRESS

tip/tilt angle of <1.5 arc second. It's believed that the HISS is stable enough for in situ interferometric testing that usually lasts less than 1 hour.

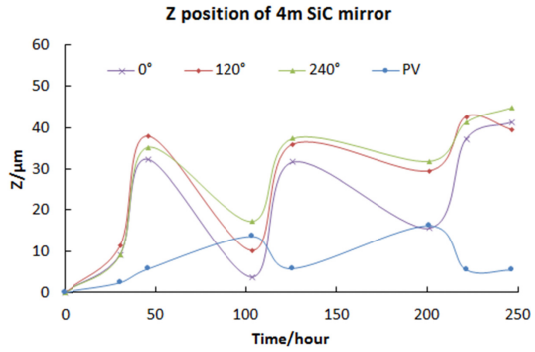

Fig. 7. Stability performance of HISS system applied to a dummy mirror.

As the real 4-m mirror is 20% lighter than the dummy mirror, it's implied that work pressure for the former would be 20% lower than the latter. Furthermore, it's also shown in Fig. 6 that the pressure drops more significantly at higher pressure, so the stability for real one would be somewhat better.

This section lays another foundation for application of HISS to large mirrors.

4. Application to a Φ4-m mirror

4.1 System integration

With the above series of analyses and tests, it's believed that the HISS system could be applied to a real 4-m mirror. According the opto-mechanical design scheme, the 4-m primary mirror is monolithic, lightweight, edge-cut (shown in Fig. 8(a)) and supported by 54 hydraulic whiffletree axial supports placed in parallel with an equal number of actuators and 24 hydraulic whiffletree lateral supports [7]. For the HISS, all the 54 HSUs are placed into 4 rings marked as R_1-R_4 from the innermost to the outermost, shown in Fig. 8(b).

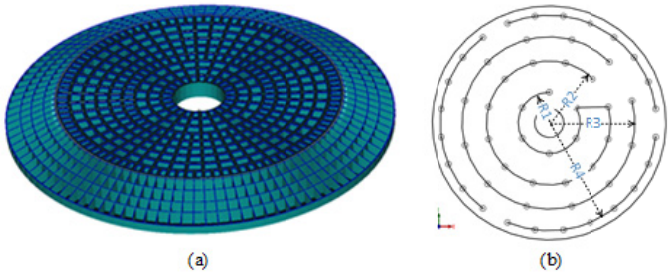

Fig. 8. Monolithic 4-m SiC mirror and its HISS: (a) mirror; (b) 5 HISS groups.

The optical shop should provide the same force boundary condition as the mirror cell during in situ optical polishing and testing process shown in Fig. 9, so the 4 rings of HSUs are assembled in 5 groups for equal force and adjustment purpose. In detail, 18 units in the R_1 and R_2 rings are linked together as trunk group 1 for equal-force purpose, 12 units in R_3 forms trunk group 2, and 24 units in R_4 are equally divided into 3 trunk groups numbered 3, 4 and 5 for tip/tilt control of the mirror. All units in the same trunk are linked in parallel as shown in Fig. 1(b).

Such grouping method brings several advantages: (1) All HSUs within a trunk work at the same inner pressure and could achieve an output force of 0.5% precision as described in

section 2.1; (2) Within each trunk group, the work fluid could run in cycle with all trunk and branch valves opened for inner air buffering to achieve high support stiffness; (3) If any HSU fails to work, substitution could be made easily by closing the corresponding input and output branch valves.

In the in situ polishing-testing iteration, the assembly should be moved along the lead rail (machine X axis) from the polishing platform (Fig. 9(a)) to the interferometric test position (Fig. 9(b)) upon the same support system precisely and stably. The custom-built 4-m scale 5-axle polishing machine named FSGJ-4000 has a platform of Φ4.5 m (much smaller than the cell of Φ6.5 m) and two arms that have interfaces for different polishing tools and could move along the machine beam (machine Y axis). The vertical (machine Z axis) space between the beam and the mirror should be larger than 1 m for polishing tools, which is impossible if the cell assembly is used in polishing. The platform has Machine C axis for workpiece rotation (used for supported mirror figure precision verification in section 5) along Z axis and Machine A axis for polishing tools.

(a) (b)

Fig. 9. Illustration for in situ polishing and testing process: (a) polishing site; (b) testing site.

As in the fabrication phase the mirror is always facing up, the lateral supports have little effect on the surface figure. So the lateral supports are simplified to 3 lateral flexible levers and 3 radial soft (relative to the mirror) pads, the former for only restraining the mirror's clock motion and the latter for restraining the mirror's XY motion. An axial HISS is specially designed because of several reasons: (1) the opto-mechanical mirror cell is too large for the platform to put on; (2) the structural design is too complex and requires long time to realize; (3) dirty optical fabrication environment will pollute all the structures involved, or even worse it may cause some key components fail to work.

Although simplified, the HISS is still rather complex, consisting of several sub-systems such as the hydraulic sub-system, the locating mechanical sub-system (lateral for the mirror and axial for each HSU), the control system and the mirror lifting-protecting system.

4.2 Figure prediction

Performance of the HISS could be evaluated in two aspects: the altitude stability and figure precision. The former could be assessed by measuring the positon of the mirror's reference surface absolutely as described in section 3. Figure precision could be simulated by FE considering the HSU's stiffness distribution within a range of ± 3% as tested in former section, and verified by in situ interferometric test.

Based on the approximate air ratio α value of 0.24% in section 2.2, the axial stiffness of group 1, group 2 and group 3-5 are predicted as 0.85 kN/mm, 1.1 kN/mm and 1.7 kN/mm respectively (by Eq. (10) and plotted in Fig. 5). With these stiffness inputs, a FE model shown in Fig. 10, coupling the mirror with the HISS, is setup by MSC.Patran for evaluating the effect of stiffness difference on mirror surface figure. Each HSU is modeled as a bush element that has an axial stiffness and a relatively small stiffness at other 5 directions, with

Optics EXPRESS

one end fixed and the other end bonded to the mirror. A gravity of G_z = –9805 mm/s^2 was set as the load during in situ testing.

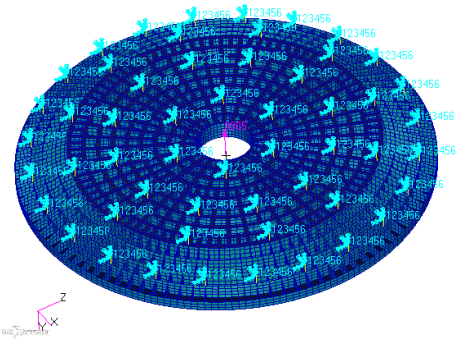

Fig. 10. Back view of the FE model representing the mirror-HISS system.

From the FE aspect, the choice of bush stiffness has a significant effect on the numerical result. Both a random distribution of ± 3% as formerly tested and an ideal case (in which all HSUs within a group have the same stiffness) were considered. After fitting the face nodes' displacements through Zernike polynomials, it's found that the largest 4 orders of aberration are rotational symmetric or astigmatic. By eliminating these orders the surface figure is shown in Fig. 11. The figure has a 20 nm RMS for the random case and 17 nm RMS for the ideal case.

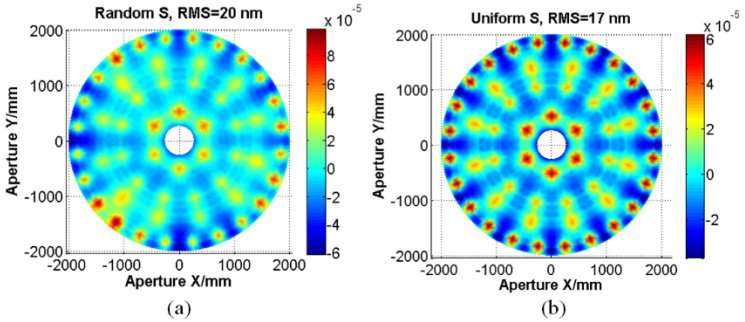

Fig. 11. Surface figure of coupled HISS-mirror system, eliminating the largest 4 order errors: (a) Random stiffness; (b) Uniform stiffness.

More detailed prediction could be performed following the same procedure, but it's not very necessary, as it could be seen form the curves in Fig. 5, for the working volume of group 1-5, the stiffness changes little when the air ratio is around 0.24%. Furthermore, stiffness difference between groups mainly produce rotational symmetric aberration which is correctable by the mirror cell.

What's more practical, figure test at different angles of the mirror relative to the HISS is always necessary, which will appear in the coming section.

5. Discussion

5.1 Precision verification

As the SiC mirror dimensions may have some unknown differences from the designed, additionally the material property is sometimes not uniform, it's very important to lift the mirror and rotate the HISS for in situ interferometric test at different clock angles for precision confirmation when necessary.

Optics EXPRESS

When the mirror was polished to the precision level of ~0.03λ RMS, HISS precision verification was carried out by testing the mirror at a clock angle of 0° and 180° relative to the HISS. In the operation, the mirror was firstly tested, uninstalled and lifted by the crane. Then the HISS was driven to the desired clock angle by the platform. Finally, the mirror was re-installed and re-tested. The tested figures were calibrated to the same angle by using of specific fiducials used for distortion correction.

Before turning, the mirror had a figure of 0.029 λ RMS, and after turning the figure was 0.033λ RMS by eliminating the power, primary spherical aberration and the astigmatism, with an absolute RMS difference of 0.004 λ and with the figure difference shown in Fig. 12.

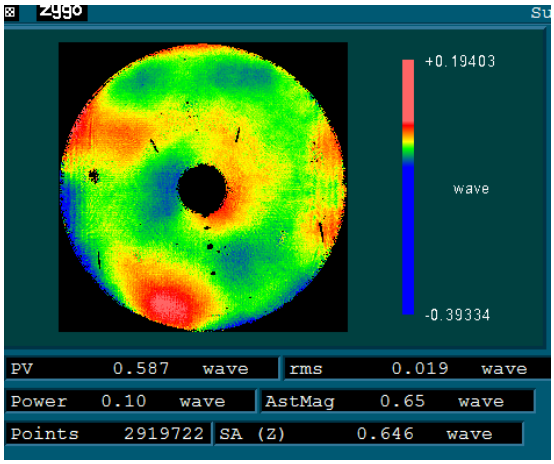

Fig. 12. Figure difference caused by the HISS rotation.

The power difference is usually not of interest, the spherical aberration difference is 0.650 λ PV with equivalent RMS of 122 nm, and the astigmatic difference is 0.646 λ PV with equivalent RMS of 83 nm. As the mirror's active support system has an ability of reducing RMS errors from 232 nm to 3 nm level within the 90% confidence interval [7], both the spherical aberration and the astigmatism are adjustable. By eliminating these two kinds of error, the residual difference between HISS transitions is 0.019 λ RMS which is comparatively small with the basic figure, showing the good precision/repetitiveness of the HISS.

But it is not telling that the system is perfect. On the other hand, some improvement could be made by using HSUs of different size as aforementioned for stiffness improvement, this will bring much smaller rotational symmetric figure errors. It's also believed that more uniform stiffness will reduce the magnitude of the astigmatism. Finer polishing and active adjustment would benefit a lot from these improvements.

5.2 Stress safety

Adjustment behavior for the aberrations tested in section 5.1 requires deformation at ~λ level, which may cause dangerous stress concentration at the mirror-structure interface, so it's very important to check the stress level of the mirror blank. The primary spherical aberration and the astigmatism tested in section 5.1 has a similar magnitude and more attention should be paid to the former one because the forces for correcting it are much bigger. Figure 13 shows the mirror's stress distribution caused by the spherical aberration predominated figure correction.

Optics EXPRESS

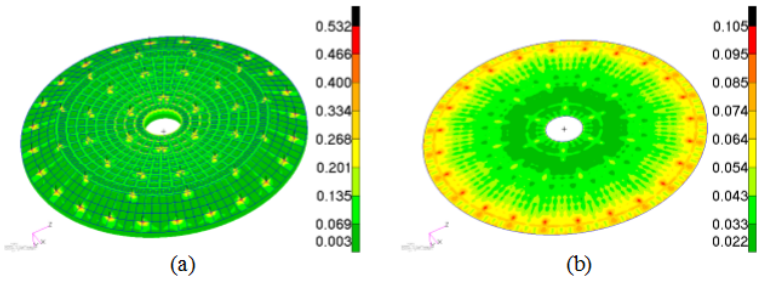

Fig. 13. Adjustment caused stress: (a) max. 0.53 MPa at back; (b) max. 0.11 MPa on the surface.

The maximum Mises stress at the interfaces is about 0.53 MPa at the outmost ring R_4, shown in Fig. 13(a). For safety consideration if a safety factor of 10 is required, it's believed that the interface stress may be as high as 5.3 MPa, which is still much lower than the strength of ~350 MPa of the SiC material, while exceeds the allowed stress of ~5 MPa for typical telescope glass [20]. And for the mirror surface shown in Fig. 13(b) the maximum stress is about 0.11 MPa and 1.1 MPa at a safety factor of 10, also much lower than the strength of optical films. So active adjustment operation for this mirror is safe enough.

5.3 Engineering effect

5.3.1 Efficiency assessment

Based on the precise and successful use of HISS, fabrication efficiency for large mirror could be greatly improved attributing to in situ polishing-testing iteration. Take the 4-m mirror for example, in an experienced mirror-turning operation, it usually needs >4 people busy working for a whole day uninstalling the mirror, moving it to the test site and re-installing it to the polishing platform.

However, with the help of HISS, in a typical 8h-polishing, 8h-moving and 1h-testing fabricating iteration, the work time decreases from 17 hours to 9 hours, bringing an efficiency improvement of 47%, and it needs just only one people for operating the platform.

5.3.2 Convenience for extension

As all the HSUs are separated from each other and easy for reconstructing, the HISS is open to arbitrary shaped workpiece and could be extended to many other fabrication processes.

What's more, through the combination of support point layout optimization, precise locating structure, use of HISS and advanced turning-milling-grinding-polishing-figuring-testing technologies, both the product precision and the project efficiency would be improved significantly.

6. Conclusion

Systematic work has been done on the HISS to support meter scale monolithic mirrors for precise in situ testing-polishing iteration. Through theoretical analysis, numerical simulation and physical test, the performance of HISS could be verified. Results shows a support force precision of 0.5%, group stiffness disparity of 3% and a slow pressure change close to the sensor's resolution.

Application to a 4-m SiC mirror shows a mirror tip/tilt angle less than 1.5″ in 10 days and that the 54-point HISS could provide a figure repetitiveness of 0.019 λ RMS with an absolute RMS difference of 0.004 λ. Both of the two main kinds of aberration appeared in the application are acceptable and correctable at a low stress level.

The HISS is a kind of precise, stable, cheap and flexible support system and would be promising in a wide field of manufacturing processes. It will improve the workpiece's

fabrication precision, safety and efficiency synchronously at a low price. Except for testing the mirror in the mirror cell at important project points, the HISS could work continuously for the in situ fabrication for most of the project time (>90%) and speed the process at a rate of 47% in a typical fabricating iteration requiring much less labor.

Also some work could be done to improve the system's performance, i.e., using different sized HSUs will lower rotational symmetric figure errors, more uniform stiffness distribution that is lower than 3% will reduce the astigmatism magnitude. It's also convinced that introducing more support units will reduce the support distance a resulting much smaller self-weight deflection proportional to a^4. The finer the process is, the more it would benefit from these improvements.

Appendix

The detailed derivation starts from Eq. (6). The diaphragm tensile force $\mathrm{d}F_\mathrm{u}$ per unit length changes by

$$\mathrm{d}F_\mathrm{u} = \frac{C\mathrm{d}P}{2} \tag{12}$$

Also from elastic mechanics, we have

$$\mathrm{d}F_\mathrm{u} = Et\frac{\mathrm{d}l}{l} \tag{13}$$

With Eqs. (12) and (13), we get $\mathrm{d}l$ by

$$\mathrm{d}l = \frac{Cl}{2Et}\mathrm{d}P \tag{14}$$

For the fluid, there's the relationship $\mathrm{d}P = -K\,\mathrm{d}V/V$, substituting $\mathrm{d}V$ with Eq. (6) it becomes

$$\mathrm{d}P = \frac{\pi RK}{V}\left[\left(R-\frac{C}{2}\right)\mathrm{d}s - \frac{C\mathrm{d}l}{2}\right] \tag{15}$$

Substituting $\mathrm{d}l$ by Eq. (14), we get

$$\mathrm{d}P = \frac{\pi RK}{V}\left[\left(R-\frac{C}{2}\right)\mathrm{d}s - \frac{C^2 l}{4Et}\mathrm{d}P\right] \tag{16}$$

and

$$\frac{\mathrm{d}P}{\mathrm{d}s} = \frac{\pi R\left(R-C/2\right)}{V/K+\pi RC^2 l/4Et} \tag{17}$$

From Eq. (5), we could get the unit's support stiffness S by

$$S = \frac{\pi^2 R^2\left(R-C\right)\left(R-C/2\right)}{V/K+\pi RC^2 l/4Et} \tag{18}$$

This is Eq. (7).

For the case where air exit within the fluid, the volume change of the air is

$$\mathrm{d}V^\mathrm{a} = -\frac{\mathrm{d}P}{P}V_0^\mathrm{a} \tag{19}$$

This volume of air is replaced by the fluid, so working fluid volume increases by

Optics EXPRESS

$$\mathrm{d}V^{\mathrm{f}} = \frac{\mathrm{d}P}{P}V_0^{\mathrm{a}} + \pi RC\left(\frac{\mathrm{d}s + \mathrm{d}l}{2}\right) - \pi R^2 \mathrm{d}s \tag{20}$$

This produce pressure change as

$$\mathrm{d}P = \frac{K}{V^{\mathrm{f}}}\left[\pi R^2 \mathrm{d}s - \pi RC\left(\frac{\mathrm{d}s}{2} + \frac{Cl}{4Et}\mathrm{d}P\right) - \frac{\mathrm{d}P}{P}V_0^{\mathrm{a}}\right] \tag{21}$$

Then we could get the stiffness by

$$S = \frac{\pi^2 R^2 (R - C)(R\text{-}C/2)}{V^{\mathrm{f}}/K + \pi RC^2 l/4Et + V_0^{\mathrm{a}}/P} \tag{22}$$

This is Eq. (10).

Funding

Ministry of Science and Technology of the People's Republic of China (National Key R and D Program 2018YFF01012400, 2016YFB0500100), National Natural Science Foundation of China (11873007, 61805243), and Jilin Department of Industry and Information Technology (Special Fund Project of Jilin Provincial Industrial Innovation 2016C030).

Acknowledgments

We gratefully thank Xiaoxia Wu and Jianfeng Li at CIOMP for the mirror cell inputs, design discussion and FE modelling help.

References

1. M. Bougoin and P. Deny, "The SiC Technology is ready for the next generation of extremely large telescopes," Proc. SPIE **4850**, 606–618 (2003).
2. X. Zhang, Z. Li, and Z. Zhang, "Space telescope aspherical mirror structure design based on SiC material," Infrared Laser Eng. **36**(5), 577–582 (2007) (in Chinese).
3. S. Liu, R. Hu, Q. Li, P. Zhou, Z. Dong, and R. Kang, "Topology optimization-based lightweight primary mirror design of a large-aperture space telescope," Appl. Opt. **53**(35), 8318–8325 (2014).
4. M. Kotani, T. Imai, H. Katayama, Y. Yui, Y. Tange, H. Kaneda, T. Nakagawa, and K. Enya, "Quality evaluation of spaceborne SiC mirrors (I): analytical examination of the effects on mirror accuracy by variation in the thermal expansion property of the mirror surface," Appl. Opt. **52**(20), 4797–4805 (2013).
5. E. Sein, Y. Toulemont, F. Safa, M. Duran, P. Deny, D. de Chambure, T. Passvogel, and G. L. Pilbratt, "A ϕ3.5 m SiC telescope for Herschel mission," Proc. SPIE **4850**, 606–618 (2003).
6. G. Zhang, W. Zhao, and R. Zhao, "Fabricating large-scale mirrors using reaction-bonded silicon carbide," SPIE Newsroom, *http://spie.org/newsroom/6582-fabricating-large-scale-mirrors-using-reaction-bonded-silicon-carbide?SSO=1.*(2016-*08-09)*.
7. B. Lan, X. Wu, J. Li, M. Ming, X. Liu, and H. Yang, "Influence of axial-force errors on the deformation of the 4 m lightweight mirror and its correction," Appl. Opt. **56**(3), 611–619 (2017).
8. H. Hu, E. Qi, X. Luo, X. Zhang, and D. Xue, "Rapid fabrication strategy for Ø1.5 m off-axis parabolic parts using computer-controlled optical surfacing," Appl. Opt. **57**(34), F37–F43 (2018).
9. E. E. Bloemhof, J. C. Lam, V. A. Feria, and Z. Chang, "Extracting the zero-gravity surface figure of a mirror through multiple clockings in a flightlike hexapod mount," Appl. Opt. **48**(21), 4239–4245 (2009).
10. L. Huang, M. Idir, C. Zuo, T. Wang, K. Tayabaly, and E. Lippmann, "Two-dimensional stitching interferometry based on tilt measurement," Opt. Express **26**(18), 23278–23286 (2018).
11. X. Wu, Y. Yu, K. Mou, and W. Wang, "In-situ stitching interferometric test system for large plano optics," Adv. Manuf. **6**(2), 195–203 (2018).
12. J. Yellowhair, P. Su, M. Novak, and J. Burge, "Fabrication and Testing of Large Flats," Proc. SPIE **6671**, 667107 (2007).
13. G. Yu, D. Walker, and H. Li, "Research on Fabrication of Mirror Segments for E-ELT," Proc. SPIE **8416**, 841602 (2012).
14. P. Shore, C. Cunningham, D. DeBra, C. Evans, J. Hough, R. Gilmozzi, H. Kunzmann, P. Morantz, and X. Tonnellier, "Precision engineering for astronomy and gravity science," CIRP Ann. Manuf. Techn. **59**(2), 694–716 (2010).
15. J. Yoder, Opto-Mechanical Systems Design, edition III (SPIE, 2006).

Optics EXPRESS

16. H. Martin, R. Allen, and B. Cuerden, "Manufacture of the second 8.4 m primary mirror for the Large Binocular Telescope," Proc. SPIE **6273**, 62730C (2006).
17. H. Hu, X. Luo, H. Xin, E. Qi, L. Zheng, and X. Zhang, "Layout optimization of equal-force supports for ultra large optical fabrication," Acta Opt. Sin. **34**(4), 0422003 (2014) (in Chinese).
18. H. Hu, E. Qi, G. Cole, H. Hu, X. Luo, V. Ford, and X. Zhang, "Hydrostatic supports for polishing TMT M3MP," Proc. SPIE **9682**, 968208 (2016).
19. L. Xiong, X. Luo, Z. Liu, X. Wang, H. Hu, F. Zhang, L. Zheng, and X. Zhang, "Swing arm profilometer: analytical solutions of misalignment errors for testing axisymmetric optics," Opt. Eng. **55**(7), 074108 (2016).
20. S. Sporer, "TMT-Stressed Mirror Polishing Fixture Study," Proc. SPIE **6267**, 62672R (2006).